

# Realization and Test of the Engineering Prototype of the CALICE Tile Hadron Calorimeter

Mark Terwort on behalf of the CALICE collaboration

**Abstract**—The CALICE collaboration is currently developing an engineering prototype of an analog hadron calorimeter (AHCAL) for a future linear collider (LC) detector. It is based on scintillating tiles that are individually read out by silicon photomultipliers (SiPMs). The prototype will contain about 2500 detector channels, which corresponds to one calorimeter layer and aims at demonstrating the feasibility of building a detector with fully integrated front-end electronics. The concept and engineering status of the prototype, as well as results from the DESY test setups are reported here.

## I. INTRODUCTION

A new engineering prototype [1] of an analog hadron calorimeter for a future experiment at an electron-positron collider is currently under development by the CALICE collaboration [2]. The aim is to build a detector with very high granularity to measure the details of hadron showers and finally separate neutral and charged particles inside a jet. Combining the energy information with the tracking information improves the energy resolution. This concept is known as *particle flow* and has been tested with testbeam data taken with the CALICE AHCAL physics prototype [3]. The development of the engineering prototype aims at the full integration of the read out electronics into the active layers of the calorimeter to minimize dead zones. It is based on scintillating tiles which are read out by silicon photomultipliers (SiPMs). The full prototype will contain 2500 detector channels (one layer) and takes into account all design aspects that are demanded by the intended operation at a LC.

A first subunit (HCAL Base Unit, HBU) with 144 detector channels has already been produced with a size of  $36 \times 36 \text{ cm}^2$ , including the scintillating tiles, four front-end low power dissipation SPIROC ASICs [4], the light calibration and gain-monitoring system and the detector/DAQ interface boards that are used for power supply as well as slow control programming. The power-supply module allows for switching off individual detector components within the LC bunch-train structure (*power pulsing*). A new data-aquisition (DAQ) has been set up, including a graphical user interface based on Labview 8.6 for comfortable test operation, while the development and testing of the final DAQ system [1] for the full prototype is still ongoing.

Currently, these HBU sub-components are redesigned in order to optimize the spatial dimensions as well as the performance of the ASICs, tiles, calibration systems and detector/DAQ interface modules to match the requirements for the integration of a full AHCAL layer. In this report the

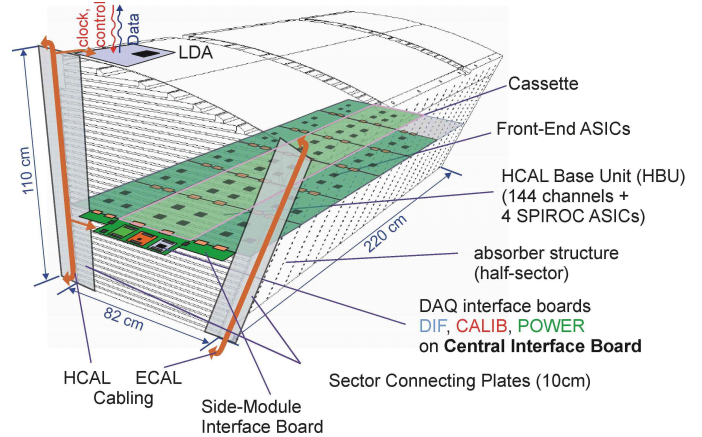


Fig. 1. 1/16 HCAL half-barrel with 48 layers containing three slabs each.

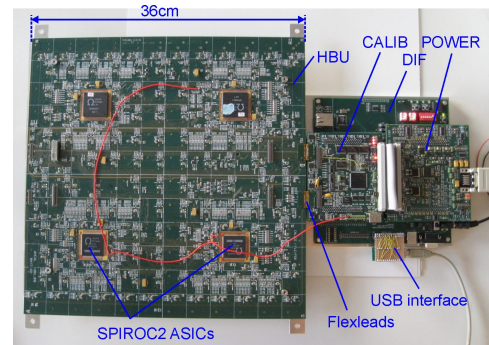


Fig. 2. Current setup of an HBU as used in the DESY test measurements.

concept of the design and results from test measurements are presented.

## II. CONCEPT AND DESIGN OF THE ENGINEERING PROTOTYPE

The barrel of the AHCAL has a cylindrical structure and will be placed outside the electromagnetic calorimeter, while it is surrounded by the magnet. The inner and outer radius is 1.8m and 2.8m, respectively. The cylindrical structure is divided into 16 segments with 48 detector layers each. One layer consists of the tiles, the embedded front-end electronics and a  $\sim 16 \text{ mm}$  thick stainless steel or  $\sim 10 \text{ mm}$  thick tungsten absorber plate. The typical size of a segment's layer is  $1 \times 2.2 \text{ m}^2$ . With 2500 channels per layer the total number of channels of the AHCAL barrel adds up to about 3.9 million.

Fig. 1 depicts the design of a single segment, showing the implementation of a specific active layer consisting of three parallel slabs. Each slab consists of six HBUs and the middle

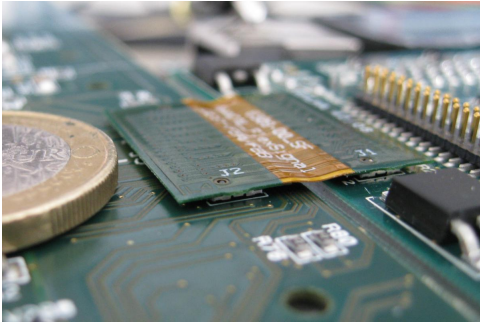


Fig. 3. HBU interconnection via flexleads and ultra-thin connectors.

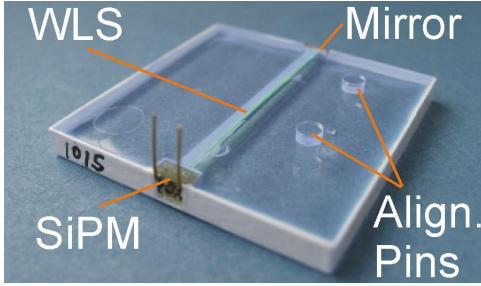


Fig. 4. Scintillating tile with embedded wavelength shifting fiber, SiPM, mirror and alignment pins.

slab is connected to the DAQ via the Central Interface Board (CIB). The side slabs are in turn connected to the CIB via the Side Interface Boards (SIBs). The first HBU module, along with the interface modules, is shown in Fig. 2, as it is used in the DESY test setups. In the final design the HBUs are interconnected by flexleads and ultra-thin connectors with a stacking height of 0.8 mm (Fig. 3), which are also used to connect the HBUs to the CIB.

One of the main new features of the embedded electronics is the on-detector zero suppression. The measurements in the testbeam will show how well this can be controlled with realistic spreads of scintillator light yields and photo-sensor gains as well as changes in environmental conditions. The chips are designed to operate with pulsed power supply for minimized heat dissipation. Establishing this operating mode under beam conditions is a major step towards establishing the integration concept for a highly granular calorimeter.

#### A. Tiles and ASICs

The signal that is detected by the SiPMs is produced by scintillating tiles with a size of  $3 \times 3 \times 0.3 \text{ cm}^3$ , as shown in Fig. 4. The new design differs from the design used in the physics prototype [5] and includes a straight wavelength shifting fiber coupled to a SiPM with a size of  $1.27 \text{ mm}^2$  on one side and to a mirror on the other side. The SiPM comprises 796 pixels with a gain of  $\sim 10^6$ . Two alignment pins are used to connect the tiles to the HBU's printed circuit board (PCB) by plugging them into holes in the PCB. The nominal tile distance is  $100 \mu\text{m}$ .

For each HBU the analog signals from the SiPMs are read out by four 36-channel ASICs equipped with 5 V DACs for a channel-wise bias voltage adjustment. They provide two

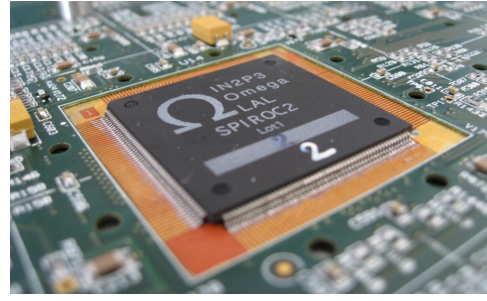


Fig. 5. Integration of the SPIROC ASIC into the PCB.

gain modes, which leads to a dynamic range of 1 to 2000 photo electrons. The foreseen power consumption amounts to  $25 \mu\text{W}$  per channel for the final LC operation. The main new features of the ASICs compared to the physics prototype are the integration of the digitization step (12-bit ADC and 12-bit TDC for charge and time measurements) and the self-triggering capability with an adjustable threshold. To reduce the height of the active layers the ASICs are lowered into the PCB by  $\sim 500 \mu\text{m}$ . This leads to a total reduction of the AHCAL diameter of 48 mm. A picture of an ASIC as it is embedded into the PCB is shown in Fig. 5.

#### B. Detector/DAQ Interface

Fig. 6 shows the cross section of one AHCAL layer including the dimensions of the single components. The active layers, including the tiles, SiPMs, PCBs and ASICs, are shown as they are placed between two layers of absorber material and connected to the CIB. The total height of the detector/DAQ interface modules hosted by the CIB has to be very small ( $\sim 18 \text{ mm}$  in case of a tungsten absorber) in order to fit between two layers. The details of the arrangement of the interface modules are shown in Fig. 7. The connections of the CIB to the SIBs and the HBUs via thin flexlead connectors are visible. The Detector Interface (DIF) serves as the interface between the inner-detector ASICs and the DAQ. The full operation via a USB-debug interface and Labview is possible and has been used in all measurements performed so far. The CALIB module controls the UV LED system, while the POWER module generates all detector supply voltages. It also enables the LC power pulsing.

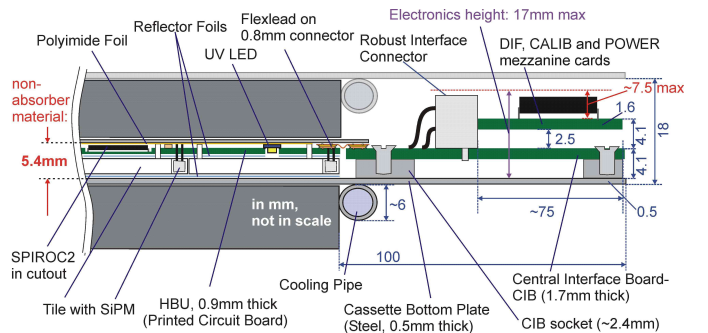


Fig. 6. Cross section of one HCAL layer, including the absorbers, tiles, SiPMs, PCBs, ASICs and the detector/DAQ interface modules. All dimensions are given in mm.

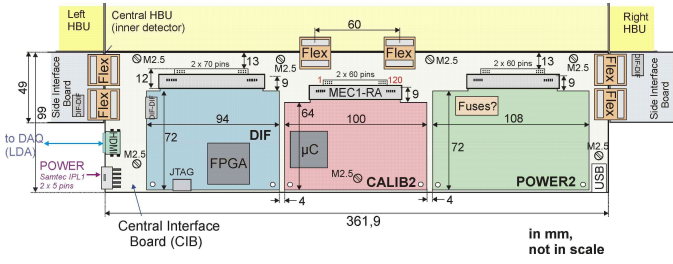


Fig. 7. Schematics of the CIB hosting the DIF, CALIB and POWER modules.

### C. Light Calibration System

Since the SiPM response shows a strong dependence on the temperature and bias voltage and saturates due to the limited number of pixels, a gain-calibration and saturation-monitoring system with a high dynamic range is needed. In the calibration mode of the ASICs a very low light intensity is needed to measure the gain as the distance between the peaks in a single-pixel spectrum, while at high light intensities (corresponding to  $\sim 100$  minimum-ionizing particles (MIPs)) the SiPM shows saturation behaviour. Currently there are two concepts under investigation:

- One LED per tile that is integrated into the detector gap (Fig. 8). This system is used in the HBUs in the DESY test setups.
- One strong LED outside the detector, while the light is distributed via notched fibers (see [6]).

Both options have been successfully tested on the DESY test setups in the laboratory and under testbeam conditions. A typical single-pixel spectrum as measured with the integrated calibration system of the test HBUs together with a fit to the gaussian peaks is shown in Fig. 9. The measured cross-talk is purely optical and is of the order of 2.5%. The dynamic range of the system redesigned for the construction of the engineering prototype is currently under investigation. The channel uniformity is also an open issue, since for the first LED system the individual LEDs have a large spread of the emitted light intensity, while for the second system the light coupling from the fiber to the tile and its mechanical integration in a full prototype is unsolved.

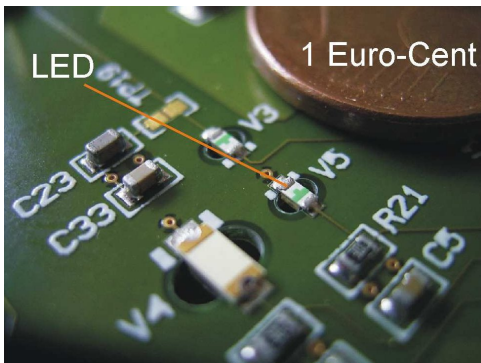


Fig. 8. Light calibration system with one integrated LED per tile.

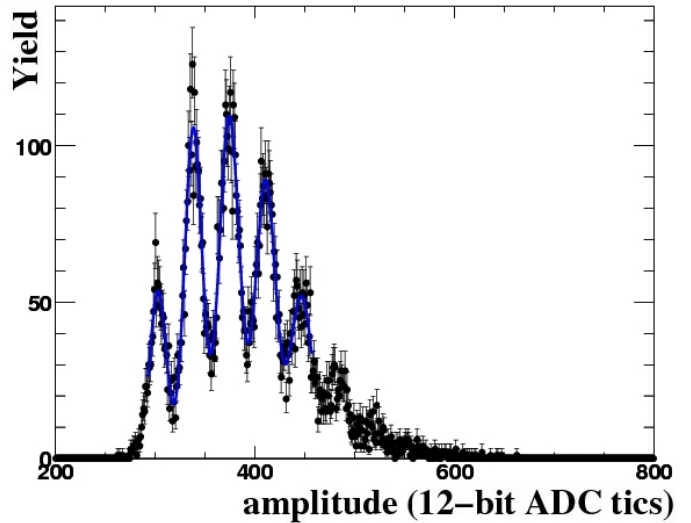


Fig. 9. Typical single-pixel spectrum as measured with the HBU in the DESY test setup. The distance between the peaks is used for the gain calibration.

## III. MEASUREMENTS AND RESULTS

The main task of the current characterization is to prove the suitability of the realized detector-module concept for the larger-scale prototype with 2500 channels and the final length of 2.2 m. Two setups as shown in Fig. 2 are in operation, one in the DESY 6 GeV electron testbeam facility (the 2-6 GeV electrons that have been used are MIPs in the scintillating tiles) and the second in a laboratory environment. A picture of the current testbeam setup is shown in Fig. 10. The HBU is enclosed into a light-tight aluminum cassette and is mounted on top of a movable stage in order to be able to scan all channels. The external beam trigger consists of two 10 cm long scintillator counters, which are placed in front of the module and are required to give coincident signals. The trigger starts the data taking on the board as far as a spill signal from the machine is present. For the results presented in the following the high gain mode of the ASIC is used with a feedback capacitance of 100 fF to couple the SiPM signal into the front-end electronics and a shaping time of 50 ns.

After the investigation of the fundamental properties like

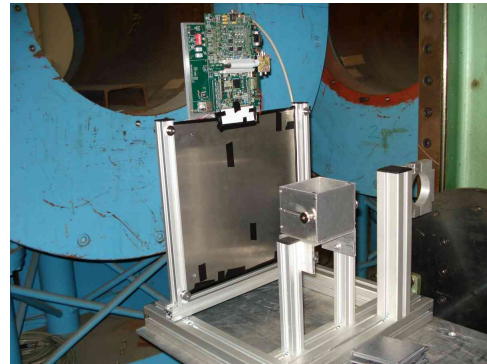


Fig. 10. The setup of the light-tight HBU cassette at the DESY testbeam is shown. On top of the cassette the CIB hosting the detector/DAQ interface modules is visible. The whole setup is mounted on a movable stage in order to be able to scan all channels.

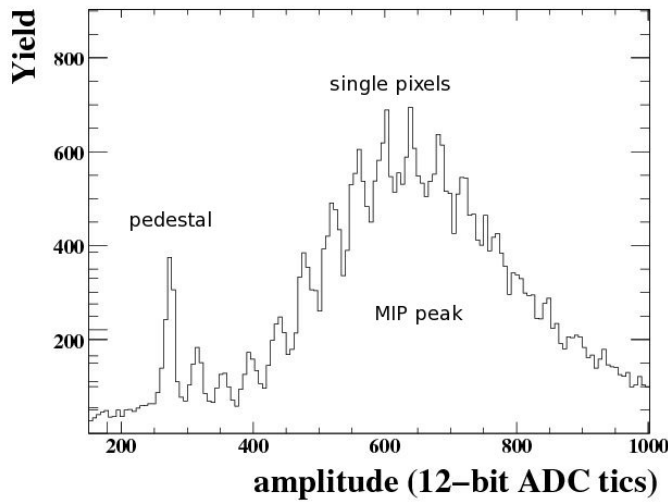


Fig. 11. Measurement result of a typical MIP spectrum obtained with the HBU and the DAQ interface modules using the newly developed Lab-view/USB DAQ in the 6 GeV DESY electron testbeam.

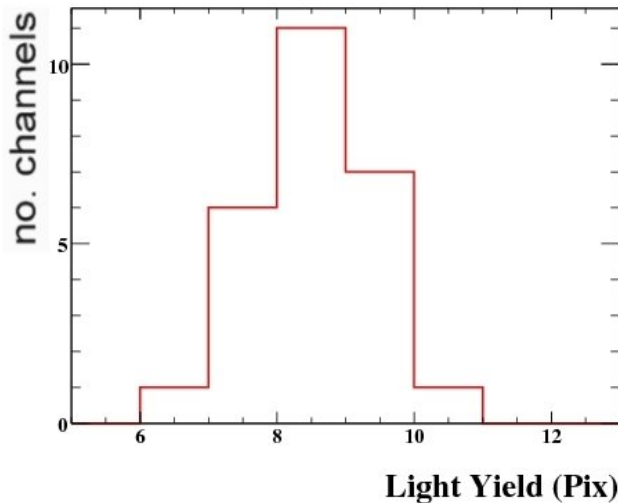


Fig. 12. Light yield as measured in the DESY testbeam facility for multiple channels of the HBU.

noise behaviour and signal delays [7], measurements in the laboratory using the LED calibration system and a charge injection setup as well as testbeam measurements have been performed to investigate the uniformity of the SiPM response as well as the behaviour of the tiles for multiple channels. Fig. 11 shows a typical MIP spectrum measured with the electron testbeam. It can be seen that single pixel peaks are clearly distinguishable for more than 10 peaks. The first peak is the pedestal peak and the maximum of the spectrum is at 9 pixels. The distribution of the light yields, defined as the most probable number of active pixels for a MIP signal, is plotted in Fig. 12.

In the following some results of the investigation of the auto-trigger are presented [8].

#### A. The Auto-Trigger

For running in a LC environment the ASICs need the capability of self-triggering (auto-triggering), since the LC

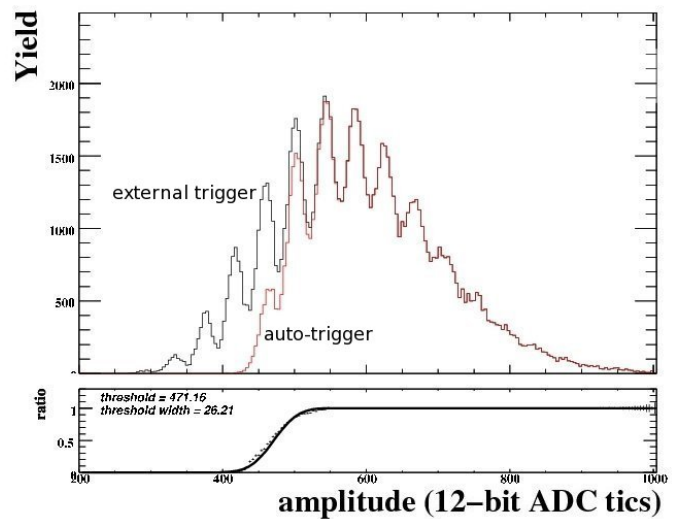


Fig. 13. Comparison of a single-pixel spectrum produced with LED light for external- and auto-triggering with a given threshold.

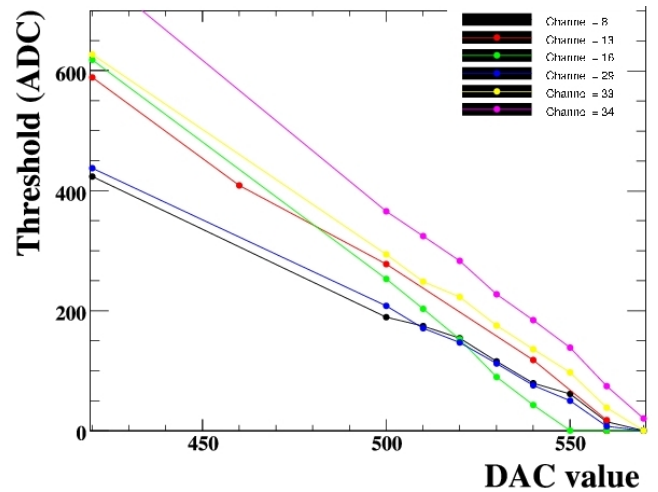


Fig. 14. Measured auto-trigger threshold as a function of the adjustable 10-bit DAC threshold. The plot shows several channels investigated with the DESY testbeam.

does not provide a central global trigger signal. Therefore the analog amplitude from the SiPM is shaped with a fast shaper (25 ns) and compared to a predefined adjustable threshold by a discriminator to make the trigger decision. Fig. 13 shows two single-pixel spectra measured with LED light and external trigger (black histogram) and auto-trigger (red histogram), respectively. The ratio of the red histogram divided by the black histogram is also shown and gives an impression of the width of the trigger turn-on curve. After the turn-on the trigger efficiency is 100%. The predefined trigger threshold used in this plot is of the order of 0.5 pC.

The behaviour of the measured threshold as a function of the predefined 10-bit DAC threshold has been investigated in charge injection as well as in testbeam measurements. Fig. 14 shows a linear behaviour for the testbeam measurement, but a significant spread among several channels in the measured threshold for a given DAC setting. This shows the necessity

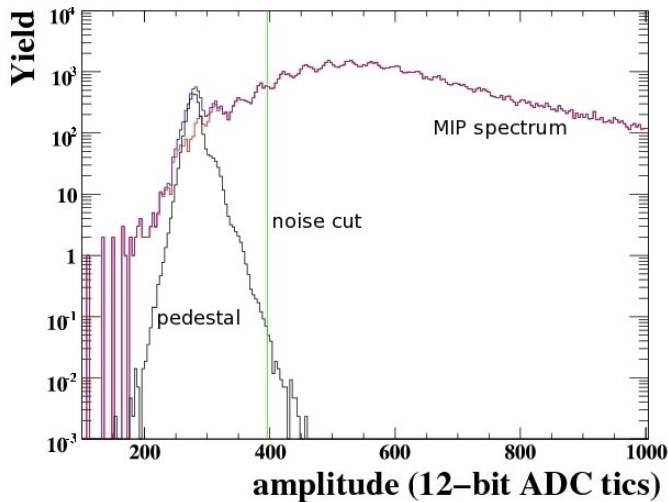


Fig. 15. Calculated auto-trigger threshold for having a noise to signal ratio of smaller than  $10^{-4}$ . An independent pedestal measurement is compared to a MIP spectrum.

of having the possibility to adjust the auto-trigger threshold channel-wise.

The threshold of the auto-trigger will be adjusted in order to minimize the noise hits and simultaneously maximize the efficiency for measuring a MIP. To investigate the distribution of the MIP efficiencies, the position of the pedestal cut has been defined such that the number of noise hits divided by the number of MIP events is smaller than  $10^{-4}$ . To calculate this, an independent noise measurement has been compared to the testbeam measurement of MIP events. Fig. 15 shows the MIP distribution (red histogram) for a given channel together with the pedestal measurement of the same channel (black histogram). The green line indicates the calculated auto-trigger threshold. With the measurement shown in Fig. 14 this threshold can be translated into a trigger threshold DAC setting for the slow control data. It turns out that a MIP efficiency of around 95% is achieved with this method. The distribution for multiple channels is shown in Fig. 16.

#### IV. CONCLUSIONS AND OUTLOOK

The CALICE collaboration is actually developing an engineering prototype for the AHCAL technology option for a possible LC experiment. It is foreseen to build a complete calorimeter layer with fully integrated front-end electronics to demonstrate the feasibility and scalability of the concepts. This requires the redesign of all involved components, including ASICs, scintillating tiles, HBUs, LED calibration systems and the detector/DAQ interface modules. The tests and measurements with charge injection, LED light and testbeams that have been performed so far, show promising results in terms of functionality and performance and lead to an increased understanding of the system. Among them are tests of the collective behaviour of many channels in terms of uniformity and interdependences as well as investigations of the behaviour of the auto-trigger.

Two of the most important next steps to be taken are tests of the power pulsing capabilities in a testbeam environment

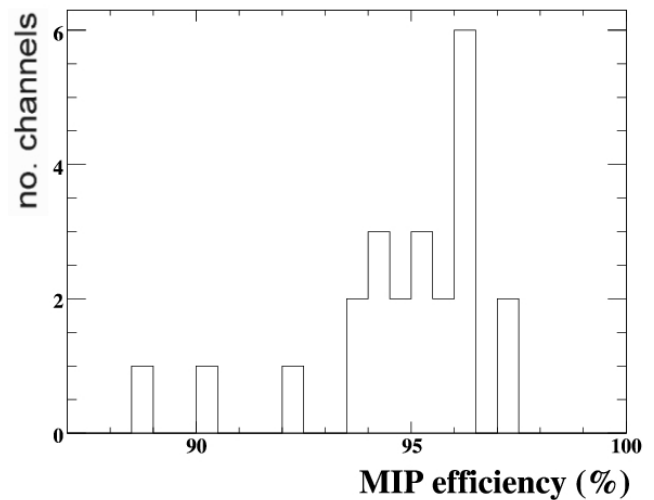


Fig. 16. Distribution of the MIP detection efficiency for a calculated auto-trigger threshold (noise to signal ratio smaller than  $10^{-4}$ ).

and the integration of the next generation DAQ. Additionally, there will be detailed studies of the TDC behaviour as well as further tests of the single next-generation components, like ASICs and tiles, to reach the performance goals required for a LC experiment.

#### V. ACKNOWLEDGMENT

The author gratefully thanks Erika Garutti, Peter Göttlicher, Mathias Reinecke, Jérémy Rouëné, Julian Sauer and Felix Sefkow for very useful discussions and valuable contributions to the results presented here. This work is supported by the Commission of the European Communities under the 6th Framework Programme “Structuring the European Research Area”, contract number RII3-026126.

#### REFERENCES

- [1] M. Reinecke et al., *Integration Prototype of the CALICE Tile Hadron Calorimeter for the International Linear Collider*, Proc. 2008 IEEE Nuclear Science Symposium (NSS08), NSSMIC.2008.4774800; T. Buanes et al., *The CALICE Hadron Scintillator Tile Calorimeter Prototype*, Proc. of Techn. and Instr. in Part. Physics (TIPP), 2009, to be published in Nucl. Instr. and Meth. A; P. Göttlicher for the CALICE collaboration, *First Results of the Engineering Prototype of the CALICE Tile Hadron Calorimeter*, Proc. 2009 IEEE Nuclear Science Symposium (NSS09), NSSMIC.2009.5402334.
- [2] CALICE home page: <https://twiki.cern.ch/twiki/bin/view/CALICE/CaliceCollaboration>
- [3] O. Markin for the CALICE collaboration, *PandoraPFA Tests using Overlaid Charged Pion Test Beam Data*, to be published in CALOR2010 proceedings.
- [4] L. Raux et al., *SPIROC Measurement: Silicon Photomultiplier Integrated Readout Chips for ILC*, Proc. 2008 IEEE Nuclear Science Symposium (NSS08), NSSMIC.2009.5401891; R. Fabbri, B. Lutz and W. Shen, *Overview of Studies on the SPIROC Chip Characterisation*, arXiv:0911.1566 and EUDET-Report-2009-05, October 2009.
- [5] C. Adloff et al., *Construction and commissioning of the CALICE analog hadron calorimeter prototype*, JINST 5 (2010) P05004, arXiv:1003.2662
- [6] I. Polák, *An LED calibration system for the CALICE HCAL*, these proceedings, 2010.
- [7] R. Fabbri for the CALICE collaboration, *CALICE Second Generation AHCAL Developments*, Proc. 2010 LCWS, arXiv:1007.2358.
- [8] J. Rouëné, *Analysis of the autotrigger of the read out chip of the front-end electronics for the HCAL of the ILC*, summer student report, 2010.